

EigenNetworks

Jonathan Mei and José M.F. Moura

Abstract—In many applications, the interdependencies among a set of N time series $\{x_{nk}, k > 0\}_{n=1}^N$ are well captured by a graph or network G . The network itself may change over time as well (i.e., as G_k). We expect the network changes to be at a much slower rate than that of the time series. This paper introduces eigennetworks, networks that are building blocks to compose the actual networks G_k capturing the dependencies among the time series. These eigennetworks can be estimated by first learning the time series of graphs G_k from the data, followed by a Principal Network Analysis procedure. Algorithms for learning both the original time series of graphs and the eigennetworks are presented and discussed. Experiments on simulated and real time series data demonstrate the performance of the learning and the interpretation of the eigennetworks.

I. INTRODUCTION

“All entities move and nothing remains still.”

—Heraclitus

In a world where change is the only constant, learning pairwise relationships among large ensembles of interacting agents from data they generate is often an interesting but difficult task. Capturing such relationships using sparse graph structures is often desired because such graphs are interpretable by humans for advancing scientific understanding [1]–[3], as well as computationally beneficial for engineering efficient analytics algorithms [4]–[7].

Assume a set of N time series $\{x_{kn}, k > 0\}_{n=1}^N$ where the dependencies are captured by time-varying networks or graphs G_k . Many network time series models treat time series as stationary, where the parameters of the model—the networks—stay constant through time $G_k \equiv G, \forall k$ [8]–[11]. We wish to extend some of these models to the non-stationary case in which these graph structures G_k themselves vary in time. Furthermore, we desire a basis that characterizes the variation of these graphs G_k with an interpretation of being somehow fundamental to the underlying process that generates the time series. In order to learn the basis, along the way we need to address the intermediate problem of estimating these time-varying networks in the first place. In this stage, we also wish to capture significant changepoints of the graphs that otherwise vary smoothly between these points if they exist.

As stated, this is a very difficult task, since we potentially need to learn a new network at every single time step! To make this vastly underdetermined problem tractable, additional assumptions are required. One common assumption takes the form that the model does not change “too quickly” (or “too often”) through time. This can be characterized with respect to some metrics for signal smoothness [12], [13]. This assumption tends to take on two primary variants: 1) bounded total variation (TV); or 2) Lipschitz temporal gradient. The

behavior of these variants can lead to strikingly different qualitative interpretations. Low total variation can be viewed as switching between networks at discrete changepoints, whereas Lipschitz gradient can be viewed as a slowly evolving network.

Since the rate of change of the networks is slow relative to the original time series, it is reasonable to believe that the graphs are well described by a time varying combination of a small set of *eigennetworks* that are fundamental to the system. This description would additionally provide a more compact summary of the process as well, reducing the total parameter size of the final learning problem. We would then ideally be able to interpret each principal network individually to make sense of the ensemble and analyze the behaviors of the interacting entities. These eigennetworks, like eigenfaces [14], span a lower dimensional subspace (“network space”) in which live the networks describing the process.

One method for enforcing smoothness on the learned model is to impose a hidden Markov model in a nonparametric Bayesian setting [15]. This model is flexible in imposing low TV by allowing the number of switched networks to be learned simultaneously with the networks themselves. However, it requires Markov Chain Monte Carlo (MCMC) sampling to learn, which provides a more detailed picture about the final learned model than a point estimate but for which convergence of the sampler is in general known to be difficult to determine [16]. Instead, we focus on optimization based approaches as the basis for our algorithms and analysis.

There have been several attempts at extending optimization methods for estimating single networks to the non-stationary setting [17], [18]. However, these methods take a black and white approach to the smoothness assumption, with either totally smooth graphs or piecewise constant graphs. We briefly introduce a modified approach for estimating time-varying graphs that allows capturing both smoothness and abrupt changepoints.

Once the time varying graphs have been learned from the time series, we would like to estimate the eigennetworks. Thinking of each graph as a vector, we see that we desire a description of a vector subspace that efficiently captures most of the variation in this set of graphs. There are myriad ways to find vectors spanning such subspaces [19]–[22]; one of the most notable examples is Principal Component Analysis (PCA) [23]. We apply a sparse version of PCA to networks and term this Principal Network Analysis (PNA).

The rest of this paper is organized as follows: section II establishes notation and reviews background; section III introduces our framework for learning smooth graphs with potential abrupt changepoints, and section IV describes the estimation of the “principal networks” from the time series of networks; section V presents experimental results of our framework on simulated and real data; and finally we conclude in section VI.

II. NOTATION AND RELATED WORKS

In this section, we will describe the models that provide foundations for the methods we consider. Much of the notation follows from [11], which estimates a single network, so we provide a brief review. We will then introduce modifications to these models to capture non-stationarity and estimate a series of time-varying networks and compare this extension with several existing methods for time varying graphs in these settings. Finally, we outline the challenges that can arise in learning these graph structures.

A. Generalized Linear Models

The Generalized Linear Model (GLM) can be described using several parameterizations. We adopt the one based on the Bregman Divergence [24], [25]. For observations $y_i \in \mathbb{R}$ and $\mathbf{x}_i \in \mathbb{R}^p$, let $\mathbf{y} = (y_1 \dots y_n)^\top$, $\mathbf{X} = (\mathbf{x}_1 \dots \mathbf{x}_n)$. The model is parameterized by 1) a non-linear link function $g = \nabla G$ for a convex function G ; and 2) a vector $\mathbf{a} \in \mathbb{R}^p$. We have the model written as

$$\mathbb{E}[y_i | \mathbf{x}_i] = g(\mathbf{a}^\top \mathbf{x}_i), \quad (1)$$

(note that some references use g^{-1} as the link function where we use g).

For data $\{\mathbf{x}_i, y_i\}$ with conditionally independent y_i given \mathbf{x}_i (note that this is not necessarily assuming that \mathbf{x}_i are independent), learning the model \mathbf{a} assuming g is known can be achieved via empirical risk minimization,

$$\hat{\mathbf{a}} = \underset{\mathbf{a}}{\operatorname{argmin}} \sum_{i=1}^n [G_*(y_i) + G(\mathbf{a}^\top \mathbf{x}_i) - y_i(\mathbf{a}^\top \mathbf{x}_i)] \quad (2)$$

where G_* is the convex conjugate of G (see [11] for further details).

B. Estimating Static Networks

First, we extend the model to the multivariate case. Let $\mathbf{y}_i = (y_{1i} \dots y_{mi})^\top$, $\mathbf{g}(\mathbf{x}) = (g_1(x_1) \dots g_m(x_m))^\top$, and $\mathbf{A} = (\mathbf{a}_1 \dots \mathbf{a}_m)^\top$. Consider the vectorization,

$$\begin{aligned} \mathbb{E}[y_{ji} | \mathbf{x}_i] &= g_j(\mathbf{a}_j^\top \mathbf{x}_i) \\ \Rightarrow \mathbb{E}[\mathbf{y}_i | \mathbf{x}_i] &= \mathbf{g}(\mathbf{A} \mathbf{x}_i). \end{aligned} \quad (3)$$

For the remainder of this paper, we make an assumption that all $g_j = g$ for notational simplicity, though the same analysis readily extends to the case where g_j are distinct.

Now, consider an additional low rank matrix coefficient \mathbf{L} in the following model,

$$\mathbb{E}[\mathbf{y}_i | \mathbf{x}_i] = \mathbf{g}((\mathbf{A} + \mathbf{L}) \mathbf{x}_i). \quad (4)$$

The matrix \mathbf{L} can be seen as incorporating the effects of some small number of latent variables \mathbf{z} on the observed variables \mathbf{x} . That is, under a true model

$$\mathbb{E}[\mathbf{y}_i | \mathbf{x}_i, \mathbf{z}_i] = \mathbf{g}(\mathbf{A} \mathbf{x}_i + \mathbf{B} \mathbf{z}_i), \quad (5)$$

the coefficient matrix \mathbf{B} induces a *low rank* \mathbf{L} additive to the *sparse* \mathbf{A} (the derivation is omitted due to space constraints; see [11] for further details). For expositional clarity, we omit \mathbf{L} , noting that we can simply substitute $\mathbf{A} \leftarrow \mathbf{A} + \mathbf{L}$ and

introduce an additional low rank regularization on \mathbf{L} in (8) below if we desire such a model.

We point out that formulating this problem as a generic regression allows us to consider graphs as either directed or undirected. To estimate directed graphs on a time series, we may for example use an autoregressive model of lag order M

$$\left\{ \begin{array}{l} \mathbf{y}_k \\ \mathbf{x}_k \\ \mathbf{A}_k \end{array} \right\} \leftarrow \left\{ \begin{array}{l} \mathbf{x}_k \\ (\mathbf{x}_{k-1}^\top \dots \mathbf{x}_{k-M}^\top)^\top \\ (\mathbf{A}_{k,1} \dots \mathbf{A}_{k,M}) \end{array} \right\} \quad (6)$$

and to estimate undirected graphs, for example,

$$\left\{ \begin{array}{l} \mathbf{y}_k \\ \mathbf{x}_k \\ \mathbf{A}_k \end{array} \right\} \leftarrow \left\{ \begin{array}{l} \mathbf{x}_k \\ \mathbf{x}_k \\ (\mathbf{1} \mathbf{1}^\top - \mathbf{I}) \odot \mathbf{A}_k \end{array} \right\} \quad (7)$$

where in row i we regress $[\mathbf{x}_k]_{\setminus i}$ (all indices of \mathbf{x}_k except for the i th) on $[\mathbf{x}_k]_i$ (the i th index of \mathbf{x}_k) by enforcing \mathbf{A}_k to have 0's on the diagonal. In general, we can also enforce any arbitrary nonzero structure $\mathbf{J} \in \{0, 1\}^{M \times N}$ on \mathbf{A}_k if we have corresponding prior structural information on the graph matrix.

When posing the learning as an optimization problem, the loss function form (2) naturally extends to the multivariate case. Other desired structural properties may be incorporated into the framework via regularization. Thus, we can pose the optimization as

$$\hat{\mathbf{A}} = \underset{\mathbf{A}}{\operatorname{argmin}} \sum_{j=1}^K f_j(\mathbf{A}) + \lambda h(\mathbf{A}) \quad (8)$$

where

$$f_j(\mathbf{A}) = \frac{1}{N} \left[\mathbf{1}^\top \left(\mathbf{G}_*(\mathbf{y}_j) + \mathbf{G}(\mathbf{A} \mathbf{x}_j) \right) - \mathbf{y}_j^\top \mathbf{A} \mathbf{x}_j \right] \quad (9)$$

Some examples for h include symmetric sparsity for sparse partial correlations (conditional independencies) in a Gaussian graphical model [26], group sparsity corresponding to sparse Granger Causality [9], and commutativity corresponding to graph filters in the Discrete Signal Processing on Graphs framework [10], [27]. More detailed discussion of different choices for regularization and their assumptions will remain beyond the scope of this paper.

C. Time-varying Networks

To further reduce clutter when convenient, we define

$$\mathcal{A} = (v(\mathbf{A}_1) \dots v(\mathbf{A}_K))^\top \in \mathbb{R}^{K \times MN}, \quad (10)$$

which collects the network-defining matrices $\mathbf{A}_k \in \mathbb{R}^{M \times N}$ through time index k , and $v(\mathbf{A})$ denotes the vectorization of a matrix \mathbf{A} . Also, we use the various shorthand forms

$$\theta_{kj} = \theta_j(\mathbf{A}_k) = \theta(\mathbf{A}_k, \mathbf{x}_j) = \mathbf{A}_k \mathbf{x}_j \quad (11)$$

so that the model is allowed to change at each time step k , and the interpretation for θ_{kj} is the linear part of the model prediction made by using the network from time k on data from time j . The actual model itself only makes sense at $k = j$, but we will see shortly why we wish to have the notational flexibility to describe these offset $k \neq j$ quantities.

Returning to our model, we have from (3) the familiar

$$\mathbb{E}[\mathbf{y}_k | \mathbf{x}_k] = \mathbf{g}(\mathbf{A}_k \mathbf{x}_k) = \mathbf{g}(\boldsymbol{\theta}_{kk}), \quad (12)$$

with a possibly non-linear link function g and an associated loss functional at time k of the general offset form

$$f_j(\mathbf{A}_k) = \frac{1}{N} \left[\mathbf{1}^\top \left(\mathbf{G}_*(\mathbf{y}_j) + \mathbf{G}(\boldsymbol{\theta}_{kj}) \right) - \boldsymbol{\theta}_{kj}^\top \mathbf{y}_j \right] \quad (13)$$

where \mathbf{G} and \mathbf{G}_* are vectorizations of G and G_* analogous to g . As currently specified, the model is overdetermined. In the following, we review assumptions from prior art that restrict the model space and make the model estimation statistically tractable.

D. Related Works

Optimization based methods also come in several flavors. One approach to impose Lipschitz gradient is to simply use a kernel estimator [17] to obtain locally stationary solutions [12] using our offset loss functionals from (13),

$$\widehat{\mathbf{A}}_k = \operatorname{argmin}_{\mathbf{A}_k} \sum_{j=1}^K w_{kj} f_j(\mathbf{A}_k) + h(\mathbf{A}_k), \quad (14)$$

where w_{kj} is the kernel weight of a symmetric kernel with some bandwidth η centered at k evaluated at j , and $h(\mathbf{A})$ is a regularizer on the sparsity of the network whose form we omit for simplicity. This is embarrassingly parallel, and allows estimating the network at a single time point without needing to compute those at other time points if deemed irrelevant. However, the smoothness of the kernel makes it more challenging to interpret for detecting discrete changepoints as the low TV setting allows.

Alternatively, an approach for enforcing low total variation [18] is to regularize the difference between neighboring time points

$$\widehat{\mathcal{A}} = \operatorname{argmin}_{\mathcal{A}} \sum_{k=1}^K f_k(\mathbf{A}_k) + \sum_{k=2}^K \|\mathbf{A}_k - \mathbf{A}_{k-1}\|_F. \quad (15)$$

This group sparse regularizer encourages the difference between networks at adjacent time points to either be all zero or non-zero. This minimization is over all networks $\mathbf{A}_1, \dots, \mathbf{A}_K$ through \mathcal{A} defined in (10). It couples the problem across time points, so that the solution is a joint estimator and is no longer so simply parallelized. Furthermore, while this model can capture significant changepoints, it is less able to describe smoother variation.

E. Local Linear Regression and Changepoints

The main conceptual workhorse for our approach is still kernel regression. However, we consider a locally linear regression instead of a vanilla kernel regression. This has the benefit of a lower bias near boundaries of the dataset, so it is natural to adopt for our purposes of changepoint detection. Changepoints can be thought of as a boundary that appears in the middle of the data; alternatively, the boundaries can be thought of as changepoints at the edges of the data domain.

The local linear regression estimator is defined similarly to the kernel estimator. For a clean signal x_k , noise signal v_k , and noisy observations $y_k = x_k + v_k$, the local linear regression estimator is

$$(\widehat{a}_k, \widehat{b}_k) = \operatorname{argmin}_{a_k, b_k} \sum_{j=1}^K w_{kj} \|y_j - (a_k + (j - k)b_k)\|_2^2, \quad (16)$$

where \widehat{a}_k is an estimate for the value of the clean signal x_k at time k , while \widehat{b}_k represents an estimate for the slope of the clean signal x_k at time k . This estimator, as compared to kernel regression, has a lower bias near the edges of the data [28].

We will be borrowing a clever use of the local linear regression [29], [30] that estimates smooth 1D signals with discrete discontinuities. They formulate several related problems with varying kernels,

$$(\widehat{a}_k^{(i)}, \widehat{b}_k^{(i)}) = \operatorname{argmin}_{a_k, b_k} \sum_{j=1}^K w_{kj}^{(i)} \|y_j - (a_k + (j - k)b_k)\|_2^2, \quad (17)$$

for $i \in \{\ell, c, r\}$ denoting left, center, and right, respectively, for which the difference between the estimators is in the kernel weights. Specifically, $w_{kj}^{(c)}$ is still a symmetric kernel centered at k evaluated at j , but

$$w_{kj}^{(r)} = \begin{cases} w_{kj}^{(c)} & j \geq k \\ 0 & j < k \end{cases} \quad (18)$$

$$w_{kj}^{(\ell)} = w_{jk}^{(r)}.$$

The intuition behind this suite of estimators is that, qualitatively, each estimator will perform best in certain settings depending on the presence and location of changepoints. Consider a single changepoint at location k' . For some small enough κ relative to the kernel bandwidth η , if $k \in [k' - \kappa, k']$, then both the right and center estimators will smooth data with two different local signal values from across the changepoint, while the left estimator will only use data with one local signal value; hence, we would expect the left estimator to be the best. Similarly, we expect the right estimator to perform best when $k \in (k', k' + \kappa]$. Finally, when there is no changepoint, we would expect the center estimator to be the best since it uses more relevant data and the underlying signal is actually smooth, matching the model assumption.

Given this intuition, how do we quantitatively decide which estimator of the three to use? At each time point, we can compute the empirical residuals of each estimator for $i \in \{\ell, c, r\}$,

$$\widehat{\epsilon}_k^{(i)} \triangleq \sum_{j=1}^K w_{kj}^{(i)} \|y_j - (a_k + (j - k)b_k)\|_2^2. \quad (19)$$

Letting $\gamma_c = \gamma \geq 0$ and $\gamma_\ell = \gamma_r = 1$, we take the index and estimator

$$I_k = \operatorname{argmin}_{i \in \{\ell, c, r\}} \gamma_i \widehat{\epsilon}_k^{(i)} \quad (20)$$

$$\widehat{a}_k = \widehat{a}_k^{(I_k)}.$$

The exact value of γ depends on assumptions about various problem settings, including those on the noise variance, minimum magnitude of the changepoints, and kernel width and

shape, just to name a few. For $\gamma = 0$, we always choose the central estimator and declare no changepoints, while for $\gamma \rightarrow \infty$ we never choose the central estimator. This range of γ values draws out the ROC for the changepoint detector. In fact, it is shown in [29], [30] that, when $\lambda = 0$, even $\gamma > 1$ implies (theoretically) never using the central estimator in the interior of the interval, and thus they advise against this. Some further practical considerations for choices of γ are discussed below equation (31) in section III-A.

F. Matrix Decompositions

Consider the problem of expressing a given matrix as the product of two matrices

$$\mathcal{A} = \mathbf{C}\mathcal{B}^\top \quad (21)$$

where $\mathcal{A} \in \mathbb{R}^{M \times N}$, $\mathbf{C} \in \mathbb{R}^{M \times R}$, and $\mathcal{B} \in \mathbb{R}^{N \times R}$ for some $R > 0$. In general, if $\text{rank}(\mathcal{A}) \leq R$ for some positive integer R , then there can be infinite solutions for the matrices \mathbf{C} and \mathcal{B} . Particular structure may be imposed on \mathbf{C} and/or \mathcal{B} to obtain desired properties or interpretations. These two matrices can be determined by any number of matrix factorization algorithms, such as a straightforward R -rank singular value decomposition in which

$$\begin{aligned} \mathcal{A} &= \mathbf{U}\Sigma\mathbf{V}^\top \\ \mathbf{C} &= \mathbf{U}\Sigma^\beta \quad \mathcal{B} = \mathbf{V}\Sigma^{1-\beta} \end{aligned} \quad (22)$$

for some choice of $\beta \in [0, 1]$, typically.

This solution can be seen as a common starting point that can give rise to other solutions, since the existence of the SVD is guaranteed while its computation is stable [31], and it yields one nice structure, with \mathbf{U} and \mathbf{V} defining orthonormal bases. However, since we expect in our application the networks to have different types of structure both temporally (smooth) and spatially (sparse), we would naturally expect any reasonably interpretable decomposition to exhibit qualitatively similar behavior. The SVD does not necessarily give us these behaviors. Thus, we consider matrix factorization techniques that can give rise to a temporally smooth \mathbf{U} and a spatially sparse \mathbf{V} (where we associate time with \mathbf{U} and network structure with \mathbf{V} indirectly via our arbitrary choice of how to stack \mathcal{A} as in (10)).

There are many algorithms for performing matrix factorization, such as probabilistic frameworks that utilize sampling [19]. Again, we focus on optimization based frameworks. Many of these tend to center around variational methods [20] or ADMM [21], [32]. Ultimately, we choose to use inertial Proximal Alternating Linear Minimization (iPALM) [33]. The iPALM method has similarities in form with ADMM, as they both utilize the separability of the objective function and computationally fast proximal operators. However, iPALM guarantees that certain types of nonconvex optimization problems, including regularized matrix factorization, converge to local minima via an adaptive choice of step size. We provide more details on implementation in section IV.

III. SMOOTH REGRESSION WITH CHANGEPONTS

We propose an optimization based approach that learns time varying graph structure jointly based on the full time series

data and attempt to bridge the gap between a smooth solution and the estimation of changepoints, as previously discussed. Our method offers the parallelizability of the previous smooth approach while being able to capturing both smooth variation and significant jumps.

A. Formulation and computation

We formulate three related locally linear regression based optimization problems,

$$(\widehat{\mathcal{A}}^{(i)}, \widehat{\mathcal{A}}'^{(i)}) = \underset{\mathcal{A}, \mathcal{A}'}{\text{argmin}} F^{(i)}(\mathcal{A}, \mathcal{A}') + \lambda h(\mathcal{A}) \quad (23)$$

for $i \in \{\ell, c, r\}$, where

$$F^{(i)}(\mathcal{A}, \mathcal{A}') \triangleq \sum_{k=1}^K \sum_{j=1}^K w_{kj}^{(i)} f_j(\mathbf{A}_k + (j-k)\mathbf{A}'_k), \quad (24)$$

and where $h(\mathcal{A})$ is a regularizer on the structure of \mathcal{A} , the $M \times N$ matrix \mathbf{A}'_k corresponds to the instantaneous time derivative¹ of \mathbf{A}_k at time k and is essentially a nuisance parameter in our setting, and the superscripts of ℓ, c, r denote left, center, and right, respectively. To reduce notational clutter, we have omitted the low-rank component, but the formulations follow exactly analogously from equation (4), by considering the additive low-rank contribution from latent variables as $\mathcal{A} \leftarrow \mathcal{A} + \mathcal{L}$ (again, see [11] for details). For $h_1(\mathcal{A})$, we can consider for example a group sparsity that corresponds to Granger causality if \mathcal{A} is autoregressive (AR) coefficient matrices, as alluded to following (8),

$$h(\mathcal{A}) = \sum_{k=M+1}^K \sum_{i,j} \|\mathbf{a}_{kij}\|_2 \quad (25)$$

where $\mathbf{a}_{kij} = ([\mathbf{A}_{k,1}]_{ij} \dots [\mathbf{A}_{k,M}]_{ij})$, the vectors collecting the ij elements of the respective AR coefficient matrices across all lag orders.

With each of these three estimators, we can see that they remain still trivially parallelizable across time points k ,

$$(\widehat{\mathbf{A}}_k^{(i)}, \widehat{\mathbf{A}}'_k) = \underset{\mathbf{A}_k, \mathbf{A}'_k}{\text{argmin}} F_k^{(i)}(\mathbf{A}_k, \mathbf{A}'_k) + \lambda h_1(\mathbf{A}_k) \quad (26)$$

where

$$F_k^{(i)}(\mathbf{A}_k, \mathbf{A}'_k) \triangleq \sum_{j=1}^K w_{kj}^{(i)} f_j(\mathbf{A}_k + (j-k)\mathbf{A}'_k) \quad (27)$$

and where $h_1(\mathbf{A}_k)$ simply acts on one of the \mathbf{A}_k .

Then following the intuition from section II-E, at each time point, we can compute the empirical residuals of each estimator for $i \in \{\ell, c, r\}$,

$$\widehat{\epsilon}_k^{(i)} \triangleq \sum_{j=1}^K w_{kj}^{(i)} f_j \left(\widehat{\mathbf{A}}_k^{(i)} + (j-k)\widehat{\mathbf{A}}'_k \right) \quad (28)$$

¹Although \mathbf{A}'_k is estimated from discrete time samples, we can still interpret it as being the continuous time derivative, since in fact we could perform this estimate in general even for non-integer values of k

In general, we can also use our favorite loss functions $D(\cdot|\cdot)$ between the estimates and the true values,

$$\tilde{\epsilon}_k^{(i)} \triangleq \sum_{j=1}^K w_{kj}^{(i)} D \left(\mathbf{g} \left(\boldsymbol{\theta}_j \left(\widehat{\mathbf{A}}_k^{(i)} + (j-k) \widehat{\mathbf{A}}_k'^{(i)} \right) \right) \middle\| \mathbf{y}_j \right). \quad (29)$$

Letting $\gamma_c = \gamma \geq 0$ and $\gamma_\ell = \gamma_r = 1$, we take the estimate

$$\begin{aligned} I_k &= \operatorname{argmin}_{i \in \{\ell, c, r\}} \gamma_i \tilde{\epsilon}_k^{(i)} \\ \widehat{\mathbf{A}}_k &= \widehat{\mathbf{A}}_k^{(I_k)}, \end{aligned} \quad (30)$$

where again γ is determined by the problem setting and in practice could be chosen via some validation procedure. Finally, the changepoints can be detected by considering the set of indices for which

$$\widehat{\mathcal{J}} = \left\{ k : (I_k = \ell) \bigcap (I_{k+1} = r) \right\}. \quad (31)$$

This tends to produce smooth behavior except near the changepoints, where the one-sided estimators are used. As an extra post-processing step, we may compute the central estimate on the boundaries of the contiguous segments to ensure smoothness in these regions.

Here, we argue that, if a quick implementation is desired, we could implicitly choose $\gamma = \infty$ by forgoing the computation of the central estimator altogether in the first pass. We would instead compare the crossover points for the errors of the left and right estimators to estimate changepoints.

Then, as a smooth solution is desired, we can run the central estimator on the contiguous segments as in the optional post-processing step described previously. This gives us one fewer parameter and lower computation at the cost of some robustness, as this requires both left and right estimators to be estimated reasonably well. Using this modification, we would detect more false changepoints that might otherwise be classified as being best fit by the central estimator under a regime for which $\gamma \leq 1$.

This intuition leads to a speedup of the original detection scheme for generic γ as well. We can first find all the potential changepoints as determined by these crossovers. Then *only* at the two time points on either side of the crossover, compute the central estimators to verify that the left and right estimators are indeed better fit than the central (i.e., that $I_k \neq 0$ for either of these points).

B. Estimation Procedure

Since our optimization problems (23) are convex, to produce our estimates, we can use any number of convex algorithms to solve the formulation. For concreteness, we provide an outline for one such approach using proximal gradient methods.

The gradient computations required are,

$$\begin{aligned} \frac{\partial F^{(i)}}{\partial \mathbf{A}_k} &\triangleq \mathbf{E}_k = \mathbf{J} \odot \sum_{j=1}^K w_{kj}^{(i)} (g(\boldsymbol{\theta}_{kj}) - \mathbf{y}_j) \mathbf{x}_j^\top \\ \frac{\partial F^{(i)}}{\partial \mathbf{A}'_k} &\triangleq \mathbf{H}_k = \mathbf{J} \odot \sum_{j=1}^K (j-k) w_{kj}^{(i)} (g(\boldsymbol{\theta}_{kj}) - \mathbf{y}_j) \mathbf{x}_j^\top \end{aligned} \quad (32)$$

where \mathbf{J} is the binary mask enforcing the 0 structure and \odot is the Hadamard or entrywise matrix product. We can let \mathcal{E} and

\mathcal{H} collect and stack $\{\mathbf{E}_k\}$ and $\{\mathbf{H}_k\}$ (respectively) the same way as \mathcal{A} collects and stacks $\{\mathbf{A}_k\}$,

$$\begin{aligned} \mathcal{E} &= (v(\mathbf{E}_1) \dots v(\mathbf{E}_K))^\top \\ \mathcal{H} &= (v(\mathbf{H}_1) \dots v(\mathbf{H}_K))^\top. \end{aligned} \quad (33)$$

Finally, we need the proximal operators for the regularizers,

$$\operatorname{prox}_1(\mathbf{A}_k, t) = \operatorname{argmin}_{\mathbf{Y}} \frac{1}{2} \|\mathbf{A}_k - \mathbf{Y}\|_F^2 + t h_1(\mathbf{Y}) \quad (34)$$

For $h_1(\mathbf{A}_k) = \sum_{i,j} \|\mathbf{a}_{kij}\|_2$, we have

$$\begin{aligned} \mathbf{S}_k &= \operatorname{prox}_1(\mathbf{A}_k, t) \\ \Rightarrow \mathbf{s}_{kij} &= \begin{cases} \left(\frac{\|\mathbf{a}_{kij}\|_2 - t}{\|\mathbf{a}_{kij}\|_2} \right) \mathbf{a}_{kij} & \|\mathbf{a}_{kij}\|_2 > t \\ 0 & \|\mathbf{a}_{kij}\|_2 \leq t \end{cases}, \end{aligned} \quad (35)$$

where the indexing of \mathbf{s}_{kij} within \mathbf{S}_k is the same as that of \mathbf{a}_{kij} within \mathbf{A}_k , which corresponds to a form of group soft thresholding that can be performed quickly.

To put it all together, algorithm 1 describes the full proximal gradient implementation.

Algorithm 1 TV Graphs using proximal gradient descent

Require: Threshold factor $\gamma > 0$, regularization parameter

$$\lambda > 0, \text{ max. iterations } t_{\max}.$$

- 1: Initialize $(\mathcal{A}^{(i)}, \mathcal{A}'^{(i)}) = (\mathbf{0}, \mathbf{0})$ or randomly, set iteration $t = 0$, initial step size s_0 .
- 2: **while** not converged and $t < t_{\max}$ **do** (in parallel over k)
- 3: Compute gradients using equation (32):

$$\mathbf{E}_k \leftarrow \frac{\partial F^{(i)}}{\partial \mathbf{A}_k} \quad \mathbf{H}_k \leftarrow \frac{\partial F^{(i)}}{\partial \mathbf{A}'_k}. \quad (36)$$

- 4: Compute proximal step

$$\begin{aligned} \mathbf{A}_k &\leftarrow \operatorname{prox}_1(\mathbf{A}_k - s_t \mathbf{E}_k, s_t \lambda) \\ \mathbf{A}'_k &\leftarrow \mathbf{A}'_k - s_t \mathbf{H}_k. \end{aligned} \quad (37)$$

- 5: $t \leftarrow t + 1$

6: **end while**

- 7: **for** $k \in \{M+1, \dots, K\}$ **do** (in parallel)

- 8: Compute empirical errors and select indices

$$\begin{aligned} \tilde{\epsilon}_k^{(i)} &= \sum_{j=1}^K w_{kj}^{(i)} D \left(\mathbf{g} \left(\boldsymbol{\theta}_j \left(\widehat{\mathbf{A}}_k^{(i)} + (j-k) \widehat{\mathbf{A}}_k'^{(i)} \right) \right) \middle\| \mathbf{y}_j \right) \\ I_k &= \operatorname{argmin}_{i \in \{\ell, c, r\}} \gamma_i \tilde{\epsilon}_k^{(i)} \\ \widehat{\mathbf{A}}_k &= \widehat{\mathbf{A}}_k^{(I_k)}, \end{aligned} \quad (38)$$

- 9: **end for**

- 10: Compute changepoints

$$\widehat{\mathcal{J}} = \left\{ k : (I_k = \ell) \bigcap (I_{k+1} = r) \right\}. \quad (39)$$

- 11: (Optional for smoothness) Compute central estimate near boundaries

- 12: **return** $\widehat{\mathcal{A}}, \widehat{\mathcal{J}}$

IV. EIGENNETWORKS: PRINCIPAL NETWORK ANALYSIS

While our method for estimating time-varying networks is fairly general, in many cases we might expect that the graphs vary in time as a linear combination of some small set of so called ‘‘Principal Networks.’’ Letting

$$\begin{aligned}\mathbf{c}_k &= (c_k^{(1)} \dots c_k^{(R)})^\top \in \mathbb{R}^{R \times 1} \\ \mathbf{C} &= (\mathbf{c}_1 \dots \mathbf{c}_K)^\top \in \mathbb{R}^{K \times R} \\ \mathbf{B}^{(r)} &\in \mathbb{R}^{M \times N} \\ \mathcal{B} &= \left(v(\mathbf{B}^{(1)}) \dots v(\mathbf{B}^{(R)}) \right) \in \mathbb{R}^{MN \times R},\end{aligned}\tag{40}$$

we can decompose a set of time varying graphs as

$$\mathcal{A} = \mathbf{C}\mathcal{B}^\top,\tag{41}$$

where \mathbf{C} collects the time-varying weights and \mathcal{B} are the vectorized Principal Networks or eigennetworks. The matrices \mathbf{C} and \mathcal{B} can be determined by any number of matrix factorization algorithms. We use an inertial version of Proximal Alternating Linearized Minimization (PALM, or iPALM for the inertial version) because of its theoretical guarantee of convergence to stationary points without requiring a tuning parameter [33], [34].

We perform matrix factorization on the output from algorithm 1 directly. Before we pose the optimization problem, we introduce the regularization to be used. For some $R > 0$, let

$$\tilde{\mathbf{A}}_k = \tilde{\mathbf{A}}(\mathcal{B}, \mathbf{c}_k) = \sum_{r=1}^R c_k^{(r)} \mathbf{B}^{(r)}.\tag{42}$$

Let our sparsity regularizer be $h_1(\mathcal{B})$. For concreteness, in the autoregressive (AR) setting we may choose a group regularization corresponding to Granger Causality,

$$h_1(\mathcal{B}) = \sum_{r=1}^R \|\mathbf{b}_{rij}\|_2\tag{43}$$

where similarly to before $\mathbf{b}_{rij} = \left(\left[\mathbf{B}_1^{(r)} \right]_{ij} \dots \left[\mathbf{B}_M^{(r)} \right]_{ij} \right)$, the vectors collecting the ij elements of the respective AR coefficient matrices across all lag orders.

Also, let our low rank regularizer be

$$h_*(\tilde{\mathcal{A}}) = \frac{1}{2} \left(\|\mathbf{C}\|_F^2 + \|\mathcal{B}\|_F^2 \right).\tag{44}$$

Now, we give the matrix factorization optimization problem,

$$\operatorname{argmin}_{\mathcal{B}, \mathbf{C}} F_{\text{mf}}(\mathcal{B}, \mathbf{C}) \triangleq \frac{1}{2} \|\tilde{\mathcal{A}} - \mathbf{C}\mathcal{B}^\top\|_F^2 + \lambda_* h_*(\tilde{\mathcal{A}}) + \lambda_1 h_1(\mathcal{B}).\tag{45}$$

The Principal Network Analysis (PNA) yields sparse \mathcal{B} that can be viewed as our eigen or principal networks, which fundamentally underlie the process and are present at any given time point in some linear combination with each other, with temporally smoothly varying weights \mathbf{C} potentially with changepoints as a result of \mathcal{A} being estimated in the same way. We could alternatively regularize \mathbf{C} to be smooth (e.g., via a grouped sparse version of Total Generalized Variation [35]) while not regularizing \mathcal{B} or even to regularize both. However, since we perform this factorization on the estimated $\tilde{\mathcal{A}}$, which

is already sparse and smooth, it is somewhat redundant and only increases the computational complexity.

To solve our nonconvex problem (45) using iPALM, we require a gradient computation on the smooth parts of the loss function and proximal operator computations for the non-smooth parts. Let

$$H(\mathcal{B}, \mathbf{C}) = \frac{1}{2} \|\tilde{\mathcal{A}} - \mathbf{C}\mathcal{B}^\top\|_F^2 + \lambda_* h_*(\tilde{\mathcal{A}}).\tag{46}$$

The gradient computations required are

$$\begin{aligned}\frac{\partial H}{\partial \mathcal{B}} &= \mathcal{Q}^\top \mathbf{C} + \lambda_* \mathcal{B} \\ \frac{\partial H}{\partial \mathbf{C}} &= \mathcal{Q}\mathcal{B} + \lambda_* \mathbf{C},\end{aligned}\tag{47}$$

where $\mathcal{Q} = \mathbf{C}\mathcal{B}^\top - \tilde{\mathcal{A}}$. To apply iPALM, we also need to compute an upper bound for the following Lipschitz constants,

$$\begin{aligned}L_{\mathcal{B}}(\mathbf{C}) &\triangleq \frac{\|\frac{\partial H}{\partial \mathcal{B}}(\mathcal{U}, \mathbf{C}) - \frac{\partial H}{\partial \mathcal{B}}(\mathcal{V}, \mathbf{C})\|_F}{\|\mathcal{U} - \mathcal{V}\|_F} \\ L_{\mathbf{C}}(\mathcal{B}) &\triangleq \frac{\|\frac{\partial H}{\partial \mathbf{C}}(\mathcal{B}, \mathbf{U}) - \frac{\partial H}{\partial \mathbf{C}}(\mathcal{B}, \mathbf{V})\|_F}{\|\mathbf{U} - \mathbf{V}\|_2}.\end{aligned}\tag{48}$$

Thus we consider

$$\begin{aligned}\left\| \frac{\partial H}{\partial \mathcal{B}}(\mathcal{U}, \mathbf{C}) - \frac{\partial H}{\partial \mathcal{B}}(\mathcal{V}, \mathbf{C}) \right\|_F &= \|(\mathcal{U} - \mathcal{V})\mathbf{C}^\top \mathbf{C} + \lambda_* (\mathcal{U} - \mathcal{V})\|_F \\ &\leq \left(\|\mathbf{C}^\top \mathbf{C}\|_F + \lambda_* \right) \|\mathcal{U} - \mathcal{V}\|_F \\ \implies L_{\mathcal{B}}(\mathbf{C}) &\leq \bar{L}_{\mathcal{B}}(\mathbf{C}) \triangleq \|\mathbf{C}\|_F^2 + \lambda_*.\end{aligned}\tag{49}$$

Similarly,

$$\begin{aligned}\left\| \frac{\partial F}{\partial \mathbf{C}}(\mathcal{B}, \mathbf{U}) - \frac{\partial F}{\partial \mathbf{C}}(\mathcal{B}, \mathbf{V}) \right\|_F &= \|(\mathbf{U} - \mathbf{V})\mathcal{B}^\top \mathcal{B} + \lambda_* (\mathbf{U} - \mathbf{V})\|_F \\ \implies L_{\mathbf{C}}(\mathcal{B}) &\leq \bar{L}_{\mathbf{C}}(\mathcal{B}) \triangleq \|\mathcal{B}\|_F^2 + \lambda_*.\end{aligned}\tag{50}$$

These upper bounds on the Lipschitz constants adaptively determine the step sizes in each coordinate block at each iteration, and thus they are slightly loose but more straightforward to compute than some other possible tighter bounds. Thus iPALM requires a bit more derivation up front to apply, but does not need tuning for step sizes, as compared to ADMM, which does not require the Lipschitz computation, but has a step size or learning rate parameter that can require properly tuning or setting in more challenging non-convex problems [21], [32].

Finally, we need the proximal operators for the regularizers,

$$\begin{aligned}\operatorname{prox}_1(\mathcal{B}, t) &= \operatorname{argmin}_{\mathcal{Y}} \frac{1}{2} \|\mathcal{B} - \mathcal{Y}\|_F^2 + t h_1(\mathcal{Y}) \\ \operatorname{prox}_s(\mathbf{C}, t) &= \mathbf{C},\end{aligned}\tag{51}$$

which can be solved quickly using soft thresholding. Putting everything together, we have algorithm 2.

We note that a natural direction for an interesting line of future work would be to combine these two steps of first estimating a time varying graph and then performing matrix factorization into a single joint formulation that directly learns the eigennetworks, or iterates between the two steps as subproblems. This could bridge the gap between a full temporally coupled solution and its computation, since the factorized form would have fewer total parameters to estimate.

Algorithm 2 PNA using iPALM with two coordinate blocks

- 1: Let $t = -1$. Set $\epsilon = \infty$, and tolerance $\delta > 0$. Overloading superscripts to denote the iteration, initialize $\mathbf{C}^{-1} = \mathbf{C}^0 = \text{rand}(K - M \times R)$ and $\mathcal{B}^{-1} = \mathcal{B}^0 = \text{rand}(MN^2 \times R)$ or with R-rank SVD.
- 2: **while** $\epsilon \geq \delta$ and $t < t_{\max}$ **do**
- 3: $t \leftarrow t + 1$
- 4: Set inertial coefficient $\zeta = \frac{t}{t+3}$
- 5: Update \mathcal{B} with fixed \mathbf{C} :
 - Use inertia: $\mathcal{Y} = \mathcal{B}^t + \zeta(\mathcal{B}^t - \mathcal{B}^{t-1})$
 - Compute gradient and Lipschitz constant for \mathcal{B} from (47) and (50):
- 6: $\mathcal{G}_b = \partial_{\mathcal{B}} F(\mathcal{Y}) \quad \bar{L}_b = \bar{L}_{\mathcal{B}}(\mathbf{C}^t)$
- 7: Apply Proximal operator from (51):

$$\mathcal{B}^{t+1} = \text{prox}_1(\mathcal{Y} - \mathcal{G}_b / \bar{L}_b, \lambda_{1,b} / \bar{L}_b)$$
- 8: Update \mathbf{C} with fixed \mathcal{B} :
 - Use inertia: $\mathbf{Z} = \mathbf{C}^t + \zeta(\mathbf{C}^t - \mathbf{C}^{t-1})$
 - Compute gradient and Lipschitz constant for \mathbf{c} from (47) and (49):
- 9: $\mathbf{G}_c = \partial_{\mathbf{C}} F(\mathbf{Z}) \quad \bar{L}_c = \bar{L}_{\mathbf{C}}(\mathcal{B}^{t+1})$
- 10: Apply Proximal operator from (51):

$$\mathbf{C}^{t+1} = \text{prox}_s(\mathbf{Z} - \mathbf{G}_c / \bar{L}_c, \lambda_{s,c} / \bar{L}_c)$$

$$= \mathbf{Z} - \mathbf{G}_c / \bar{L}_c$$
- 11: Compute error

$$\epsilon \leftarrow \left\| \begin{pmatrix} \mathcal{B}^{t+1} \\ \mathbf{C}^{t+1} \end{pmatrix} - \begin{pmatrix} \mathcal{B}^t \\ \mathbf{C}^t \end{pmatrix} \right\|_F / \left\| \begin{pmatrix} \mathcal{B}^t \\ \mathbf{C}^t \end{pmatrix} \right\|_F$$
- 12: **end while**
- 13: **return** $(\mathcal{B}^t, \mathbf{C}^t)$

V. EXPERIMENTS

We test the time varying graph estimation on simulated and real data sets. We perform principal network analysis on the results of a US Senate voting record data set to yield the principal networks that we show has interpretable meaning in the context of the contemporary political climate.

A. Simulated Data

We generated networks of size $N \in \{25, 50\}$ of length $K \in \{100, 250\}$. We generated \mathbf{A} randomly as Erdős-Rényi in structure and $\mathcal{N}(0, 1)$ in weight with a diagonal uniformly generated in $[1, 2]$. We generate the time-varying weights as piecewise constants with magnitude generated uniformly at random in $[2, 4]$ plus a sinusoid of magnitude also generated uniformly at random in $[1/4, 1/2]$, in which changepoints are generated uniformly at random in $\left[\frac{K-M}{R+1}(i - \frac{1}{8}), \frac{K-M}{R+1}(i + \frac{1}{8})\right]$ for $i = 1, \dots, R$ where R is the number of changepoints. This is a fairly difficult setting conceptually, as the non-zero structure of the graphs is actually constant throughout the duration of the time series as all of the true underlying graphs are present, but the magnitudes change, so that the changepoints

are jumps in magnitude rather than structural changes in existence of edges. In figure 1, we see that the near the detected

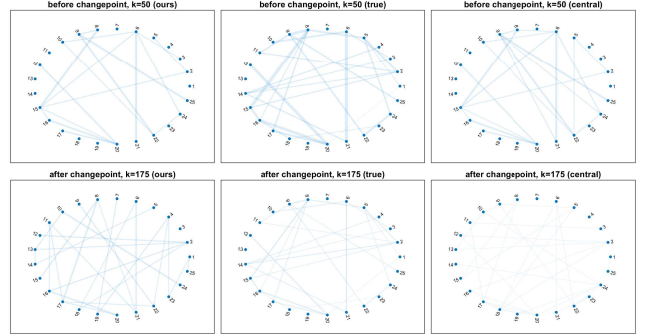


Fig. 1: Graphs of the top 50 edges

changepoint, using the same sparsity regularization parameter λ , the networks estimated with the changepoints are better able to capture the weights on either side of the changepoint, while the central estimator seems to average too strongly across the changepoint, resulting in weaker edges. We show in figure 2

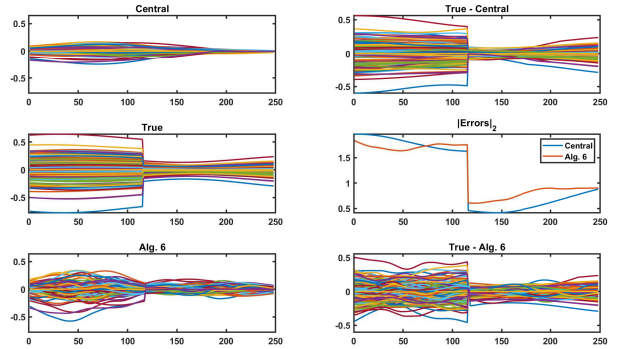


Fig. 2: Time series of elements of graph adjacency matrix and corresponding errors

the performance of our estimation method as compared to the central estimator for $\lambda = 0.1$ and $w_{kj}^{(c)} \propto e^{-\frac{(j-k)^2}{200}}$. In figure 2 each line represents the time series of the weights corresponding to one edge. There are 10000 such lines. We see that using our method, the changepoint is estimated well, and the overall error (middle right) is less than that of the normal central kernel estimate. We note that the estimated magnitudes of the edge weights for the graph are shrunk as a result of the regularization, and also that there is still some bias towards 0 at the boundaries (i.e., that the magnitudes of the nonzero entries in the estimated edge weights are systematically lower). This suggests an extension of the method would be to let the regularization parameter λ vary through the interval rather than stay constant. A proper time profile of the λ value would be of interest.

B. US Senate Voting Data

We also compiled $K = 500$ votes from the United States senate roll call records of sessions 111-112, corresponding to

a period from 2010-2011 [36], [37]. There are 2 senators from each of 50 states, so that there are at most $N = 100$ senators voting on each item. However, instead of directly tracking a growing and shrinking network composed of individual senators, we track the seat that the senator occupies, so that the time series of votes generated by senators continue being produced by their replacements. We treat yes votes as $+1$, no votes as -1 , and abstentions/vacancies as 0 so that the time series is $\mathbf{X} \in \{-1, 0, +1\}^{100 \times 500}$ (see figure 3).

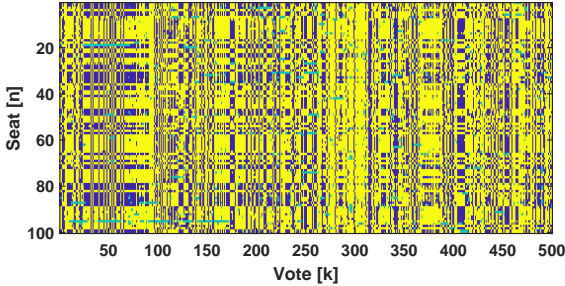


Fig. 3: Time series of votes by seat, yellow (dominant color) (+1) for Yea, blue (dark) (-1) for Nay, and green (light) (0) for abstention/vacant seat.

TABLE I: Examples of unanimous/procedural votes

Yea - Nay	Outcome	Purpose
97 - 0	Agreed to	A resolution honoring the victims and heroes of the shooting...in Tucson, Arizona.
96 - 1	Agreed to	...to provide penalties for aiming laser pointers at airplanes...
100 - 0	Confirmed	Confirmation Robert S. Mueller, III, of California, to be Director of the Federal Bureau of Investigation
0 - 97	Rejected	...budget request for the United States Government for fiscal year 2012, and...budgetary levels for fiscal years 2013 through 2021.

Since a significant portion of votes is nearly unanimous and/or procedural as according to senate rules, as opposed to actually debated and/or legislative and thus truly informative, it is unclear that modeling the effect that temporally neighboring votes have on each other is more meaningful than recovering the reciprocal relations (at least using the frameworks presented in this chapter). For some examples of such unanimous or procedural votes, see table I [37]. Thus, we apply the undirected graph estimation model from equation (7) with the low-rank component included to track the network of relations among the senate.

We use a slightly different sparsity regularization to account for the symmetric structure of the adjacency matrix to be estimated,

$$h(\mathcal{A}) = \sum_k \sum_{i < j} \|(\mathbf{A}_k)_{ij} (\mathbf{A}_k)_{ji}\|_2.$$

We see at the top of figure 4 the $N^2 = 10^4$ individual elements of the estimated adjacency matrix, one color for each ij entry plotted as a function of time k . In the middle, we see that the algorithm detected a changepoint at timepoint

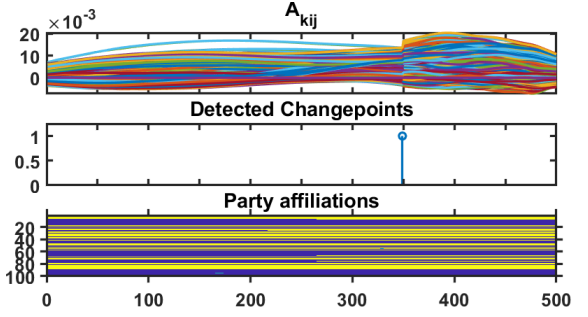


Fig. 4: Top: time series of entries of estimated graph adjacency. Each color is one time element of the matrix. Middle: Changepoints detected by algorithm. Bottom: Actual party affiliations for each seat, yellow (light) for Republican, blue (dark) for Democrat.

349. In the bottom of the figure, we see evidence that there was actually the start of a new session (transition from 111-112) at timepoint 264 (Jan. 2011) in which 5 new senators were elected of the opposite political party to the previous senator they replaced (Republicans replacing Democrats). This happened as the so-called “Tea Party,” which started as a vocal grassroots movement and was active in organizing national demonstrations, had gained major traction in the US Republican Party [38]. However, there is a significant lag in the detection of this changepoint. We conjecture that this is due to the large segment of largely uninformative unanimous votes in the beginning of the new session (see figure 3) that were predicted equally well (or poorly) under either left or right model.

In figures 5 and 6, we compare estimated networks using our method and the central kernel estimate from $k = 175$ and $k = 425$, corresponding to two points respectively before and after the start of the new session as well as the detected changepoint. The top layouts are achieved by using a planar force-directed embedding based on the edges estimated in $\hat{\mathbf{A}}_k$ (in particular, we use the Fruchterman-Reingold [39] layout as implemented in MATLAB® version 2018a). Intuitively, shorter average path lengths between nodes correspond to larger forces and lower distances in the planar embedding. The bottom layouts are computed using the top layouts as initialization points. Neighboring points vote more similarly, signifying ideological closeness. We additionally label seats according to the ground truth party of the senator occupying them at that time, with Republicans in red, Democrats in blue, and the Independent in yellow.

In figure 5, we can see that the graph clearly shows the polarization between the two parties. Interestingly, the Independent is shown as ideologically closer to the democrats but on the closest edge to the Republicans. Indeed, the Independent is Senator Sanders, whom we know to hold views that are espoused by both parties, but in 2016 ultimately ran in the Democratic primary race to try to become the party’s presidential candidate. In addition, we point out two seats, 7 (Arkansas) and 27 (Indiana) who were Democratic prior to the election, but switched to Republican afterwards. These senators were on the boundary of the Democratic cluster

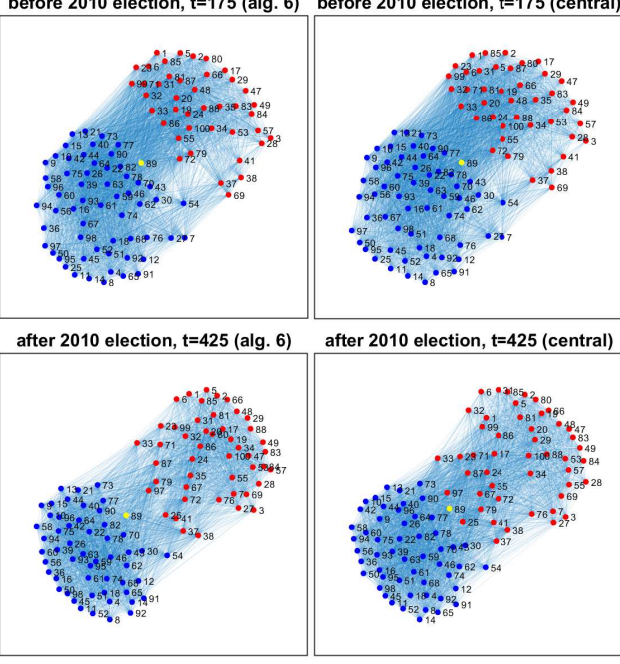


Fig. 5: Top: Estimated adjacency graph from middle of first session; Bottom: Estimated adjacency graph from middle of second session; Left: Our method; Right: Central estimator

to begin with, which is consistent with the fact that both states historically lean Republican as measured by the previous 8 presidential elections (2008 was in fact an exception for Indiana, while 1992 and 1996 were exceptions for Arkansas as the Democratic candidate was from Arkansas) [40], [41]. Also, we note that the shapes of the clusters change, with the Democratic clique flattening while the Republican clique stretches. We must be careful in drawing any conclusions from this phenomenon, but this could weakly support (i.e., not provide any evidence to disprove) the conclusions drawn by political researchers claiming that official recognition of the “Tea Party Movement” and its unity resulted in the Republican Party moving ideologically further away from the previous center of the political space [42], [43]. Finally, we see that the two methods estimate very similar graphs, showing that our method performs a similar estimation to the smooth central kernel estimator in regimes away from changepoints.

In figure 6, we visualize graphs estimated on either side of the detected changepoint at $k = 349$, this time much closer to the changepoint. We see that the central kernel shows less change between the two timepoints, while there is a noticeable difference across the changepoint in our method. In the top row, there is also some movement relative to the timepoints visualized in figure 5, possibly corresponding to posturing ahead of the election. Continuing our previous interpretations, this could be the existing Republicans trying to maintain their seats over “Tea Party” primary challengers [42]. We clarify one subtlety on this theory: though the visualized timepoint is actually *after* the beginning of the new session, the kernel bandwidth is such that the votes from *before* in the old session still influence the estimated graph in both methods,

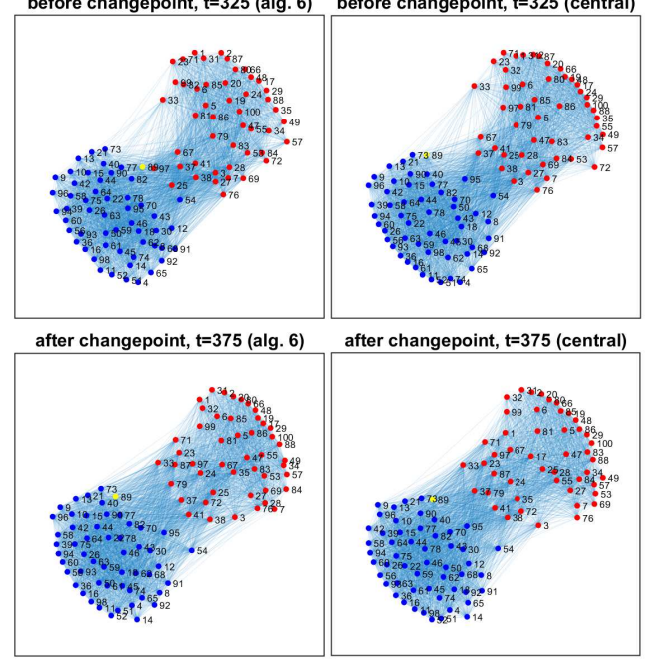


Fig. 6: Top: Estimated adjacency graph from the first session near the detected changepoint; Bottom: Estimated adjacency graph from the second session near the detected changepoint; Left: Our method; Right: Central estimator

as the visualized timepoint still occurs before the *detected* changepoint.

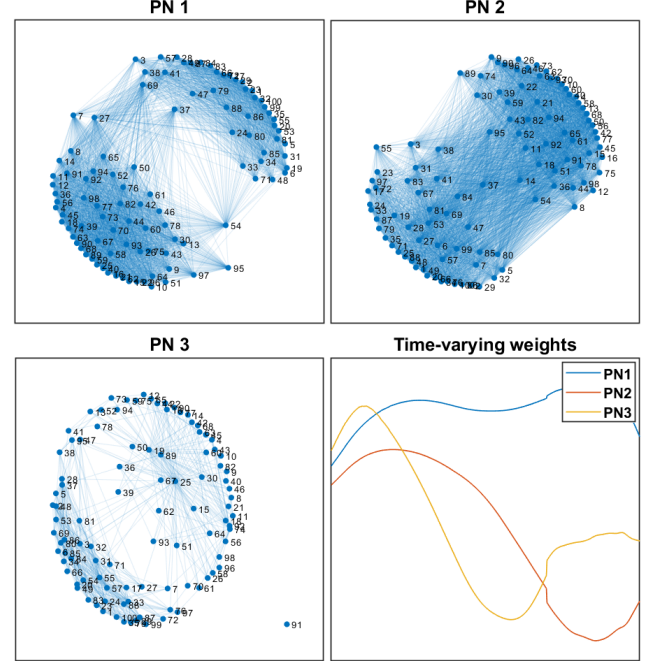


Fig. 7: Eigennetworks (EN) or Principal Networks (PN) of the senate voting record; Bottom-right: relative time-varying weights for each network

Finally, in figure 7 we visualize the result of PNA applied

to this dataset, again using a force-directed layout. This time, note that we do not label the nodes by color since these networks are now across all time, so several seats could be either red or blue depending on the time. We find that the first two Eigennetworks (EN) or Principal Networks (PN) capture the main overall polarized structure of the two parties. EN 3, on the other hand, seems to highlight the most salient and influential seats in the senate. In this case, we see visually that the time series for EN 3 has the largest time derivatives, so that the network corresponds to the edges that had the largest changes throughout the dataset. Again, Independent senator Sanders (89) is seen towards the interior of the network, indicating the existence of many edges with many seats with all manner of ideologies. We see that seat 25 is also towards the center of this network. Interestingly, this is Democratic senator Burris from Illinois, who was specially appointed by the governor as a result of then-senator Obama's resignation after his election to the presidency in 2008, who retired prior to the beginning of the new session to be replaced by Republican senator Kirk. This change in ideologies occurring before the single detected changepoint was clearly not large enough in magnitude to result in another changepoint, but rather it led to the seat seeming to share ideologies across both parties and a strong presence in EN 3 as a seat with many large enough edges changing smoothly.

VI. CONCLUSION

We have presented a framework for learning the eigennetworks— a small set of fundamental graphs— that underlie a system described by smooth graphs with potential changepoints. This framework includes a time-varying graph estimation method and a Principal Network Analysis. The graph estimation is easily parallelized, as a middle ground to existing methods for estimating time-varying graphs. The Principal Network Analysis is provably convergent and finds the fundamental graphs that we term eigennetworks. We demonstrate the use of this framework on simulated data as well as real US senate voting records for identifying interesting entities within the network and the times at which salient events occurred.

An interesting direction for future work includes developing additional guarantees for each step of the approach and thus observing the propagation of error through the two steps. Additionally, the application of this method to other areas of science would be exciting, especially in budding areas of neuroscience. A final area of interest is in combining the frameworks for learning graph time series and the Principal Network Analysis into a single problem in a numerically stable algorithm, again with performance guarantees.

REFERENCES

- [1] G. Deshpande, P. Santhanam, and X. Hu, "Instantaneous and causal connectivity in resting state brain networks derived from functional MRI data," *NeuroImage*, vol. 54, no. 2, pp. 1043–1052, Jan. 2011. [Online]. Available: <http://www.sciencedirect.com/science/article/pii/S105381191001205X>
- [2] K. Sachs, O. Perez, D. Pe'er, D. A. Lauffenburger, and G. P. Nolan, "Causal Protein-Signaling Networks Derived from Multiparameter Single-Cell Data," *Science*, vol. 308, no. 5721, pp. 523–529, Apr. 2005. [Online]. Available: <http://www.sciencemag.org/content/308/5721/523>
- [3] P. A. Valdés-Sosa, J. M. Sánchez-Bornot, A. Lage-Castellanos, M. Vega-Hernández, J. Bosch-Bayard, L. Melie-García, and E. Canales-Rodríguez, "Estimating brain functional connectivity with sparse multivariate autoregression," *Philos. Trans. R. Soc. Lond. B. Biol. Sci.*, vol. 360, no. 1457, pp. 969–81, May 2005. [Online]. Available: <http://www.pubmedcentral.nih.gov/articlerender.fcgi?artid=1854937&tool=pmcentrez&rendertype=abstract>
- [4] S. T. Roweis and L. K. Saul, "Nonlinear Dimensionality Reduction by Locally Linear Embedding," *Science*, vol. 290, no. 5500, pp. 2323–2326, Dec. 2000. [Online]. Available: <http://www.sciencemag.org/content/290/5500/2323>
- [5] O. Livne and A. Brandt, "Lean Algebraic Multigrid (LAMG): Fast Graph Laplacian Linear Solver," *SIAM Journal on Scientific Computing*, vol. 34, no. 4, pp. B499–B522, Jan. 2012. [Online]. Available: <https://pubs.siam.org/doi/abs/10.1137/110843563>
- [6] A. Khan, N. Li, X. Yan, Z. Guan, S. Chakraborty, and S. Tao, "Neighborhood Based Fast Graph Search in Large Networks," in *Proceedings of the 2011 ACM SIGMOD International Conference on Management of Data*, ser. SIGMOD '11. New York, NY, USA: ACM, 2011, pp. 901–912. [Online]. Available: <http://doi.acm.org/10.1145/1989323.1989418>
- [7] Y. Boykov, O. Veksler, and R. Zabih, "Fast approximate energy minimization via graph cuts," *IEEE Transactions on Pattern Analysis and Machine Intelligence*, vol. 23, no. 11, pp. 1222–1239, Nov. 2001.
- [8] F. R. Bach and M. I. Jordan, "Learning graphical models for stationary time series," *IEEE Transactions on Signal Processing*, vol. 52, no. 8, pp. 2189–2199, Aug. 2004.
- [9] A. Bolstad, B. Van Veen, and R. Nowak, "Causal network inference via group sparse regularization," *IEEE Transactions on Signal Processing*, vol. 59, no. 6, pp. 2628–2641, Jun. 2011.
- [10] J. Mei and J. M. F. Moura, "Signal processing on graphs: causal modeling of unstructured data," *IEEE Transactions on Signal Processing*, vol. 65, no. 8, pp. 2077–2092, Apr. 2017.
- [11] ———, "SILVar: Single index latent variable models," *IEEE Transactions on Signal Processing*, vol. 66, no. 11, pp. 2790–2803, Jun. 2018.
- [12] R. Dahlhaus, "Locally stationary processes," *Handbook of statistics*, vol. 30, pp. 351–412, 2012. [Online]. Available: <https://books.google.com/books?hl=en&lr=&id=9wXOytMWHQoC&oi=fnd&pg=PA351&dq=locally+stationary+processes+dahlhaus&ots=5iSnYa6gZM&sig=c2dndyjRfnKwKMq-dy7bv1WD-Yw>
- [13] A. Chambolle, "An Algorithm for Total Variation Minimization and Applications," *Journal of Mathematical Imaging and Vision*, vol. 20, no. 1-2, pp. 89–97, Jan. 2004. [Online]. Available: <https://link.springer.com/article/10.1023/B:JMIV.0000011325.36760.1e>
- [14] M. A. Turk and A. P. Pentland, "Face recognition using eigenfaces," in *1991 IEEE Computer Society Conference on Computer Vision and Pattern Recognition Proceedings*, Jun. 1991, pp. 586–591.
- [15] A. S. Willsky, E. B. Sudderth, M. I. Jordan, and E. B. Fox, "Nonparametric Bayesian Learning of Switching Linear Dynamical Systems," *Advances in Neural Information Processing Systems (NIPS) 21*, pp. 457–464, 2009, editors: D. Koller, D. Schuurmans, Y. Bengio and L. Bottou. Publisher: Curran Associates, Inc.
- [16] C. Andrieu, N. de Freitas, A. Doucet, and M. I. Jordan, "An Introduction to MCMC for Machine Learning," *Machine Learning*, vol. 50, no. 1-2, pp. 5–43, Jan. 2003. [Online]. Available: <https://link.springer.com/article/10.1020281327116>
- [17] L. Song, M. Kolar, and E. P. Xing, "Time-Varying Dynamic Bayesian Networks," in *Advances in Neural Information Processing Systems 22*, Y. Bengio, D. Schuurmans, J. D. Lafferty, C. K. I. Williams, and A. Culotta, Eds. Curran Associates, Inc., 2009, pp. 1732–1740. [Online]. Available: <http://papers.nips.cc/paper/3716-time-varying-dynamic-bayesian-networks.pdf>
- [18] M. Kolar and E. P. Xing, "Estimating networks with jumps," *Electronic journal of statistics*, vol. 6, pp. 2069–2106, 2012. [Online]. Available: <http://www.ncbi.nlm.nih.gov/pmc/articles/PMC4085697/>
- [19] R. Salakhutdinov and A. Mnih, "Bayesian probabilistic matrix factorization using Markov chain Monte Carlo," in *In ICML 08: Proceedings of the 25th International Conference on Machine Learning*, 2008.
- [20] D. Dueck and B. Frey, "Probabilistic sparse matrix factorization," *Univ. Toronto Tech. Rep. PSI-2004*, 2004. [Online]. Available: <http://www.psi.toronto.edu/psi/pubs/2004/PSI-TR-2004-23.pdf>
- [21] D. Hajinezhad, T. H. Chang, X. Wang, Q. Shi, and M. Hong, "Nonnegative matrix factorization using ADMM: Algorithm and convergence analysis," in *2016 IEEE International Conference on Acoustics, Speech and Signal Processing (ICASSP)*, Mar. 2016, pp. 4742–4746.

[22] E. J. Candès, X. Li, Y. Ma, and J. Wright, "Robust Principal Component Analysis?" *J. ACM*, vol. 58, no. 3, pp. 11:1–11:37, Jun. 2011. [Online]. Available: <http://doi.acm.org/10.1145/1970392.1970395>

[23] S. Wold, K. Esbensen, and P. Geladi, "Principal component analysis," *Chemometrics and Intelligent Laboratory Systems*, vol. 2, no. 1, pp. 37–52, Aug. 1987. [Online]. Available: <http://www.sciencedirect.com/science/article/pii/0169743987800849>

[24] L. M. Bregman, "The relaxation method of finding the common point of convex sets and its application to the solution of problems in convex programming," *USSR Computational Mathematics and Mathematical Physics*, vol. 7, no. 3, pp. 200–217, Jan. 1967. [Online]. Available: <http://www.sciencedirect.com/science/article/pii/0041555367900407>

[25] A. Banerjee, S. Merugu, I. S. Dhillon, and J. Ghosh, "Clustering with Bregman divergences," *Journal of Machine Learning Research*, vol. 6, no. Oct, pp. 1705–1749, 2005. [Online]. Available: <http://www.jmlr.org/papers/v6/banerjee05b.html>

[26] J. Friedman, T. Hastie, and R. Tibshirani, "Sparse inverse covariance estimation with the graphical Lasso," *Biostatistics*, vol. 9, no. 3, pp. 432–41, Jul. 2008. [Online]. Available: <http://www.pubmedcentral.nih.gov/articlerender.fcgi?artid=3019769&tool=pmcentrez&rendertype=abstract>

[27] A. Sandryhaila and J. M. F. Moura, "Discrete Signal Processing on Graphs," *IEEE Transactions on Signal Processing*, vol. 61, no. 7, pp. 1644–1656, Apr. 2013.

[28] J. Fan and I. Gijbels, "Local linear smoothers in regression function estimation," North Carolina State University, Technical Report 2055, 1991.

[29] P. Qiu, "A jump-preserving curve fitting procedure based on local piecewise-linear kernel estimation," *Journal of Nonparametric Statistics*, vol. 15, pp. 437–453, 2003.

[30] I. Gijbels, A. Lambert, and P. Qiu, "Jump-preserving regression and smoothing using local linear fitting: a compromise," *Annals of the Institute of Statistical Mathematics*, vol. 59, pp. 235–272, 2007.

[31] L. N. Trefethen and D. Bau III, *Numerical Linear Algebra*. SIAM, Jan. 1997, google-Books-ID: JaPtxOytY7kC.

[32] S. Boyd, N. Parikh, E. Chu, B. Peleato, and J. Eckstein, "Distributed optimization and statistical learning via the alternating direction method of multipliers," *Found. Trends Mach. Learn.*, vol. 3, no. 1, pp. 1–122, Jan. 2011. [Online]. Available: <http://dx.doi.org/10.1561/2200000016>

[33] T. Pock and S. Sabach, "Inertial proximal alternating linearized minimization (iPALM) for nonconvex and nonsmooth problems," *SIAM Journal on Imaging Sciences*, vol. 9, no. 4, pp. 1756–1787, Jan. 2016. [Online]. Available: <https://pubs.siam.org/doi/10.1137/16M1064064>

[34] J. Bolte, S. Sabach, and M. Teboulle, "Proximal alternating linearized minimization for nonconvex and nonsmooth problems," *Mathematical Programming*, vol. 146, no. 1-2, pp. 459–494, Aug. 2014. [Online]. Available: <https://link.springer.com/article/10.1007/s10107-013-0701-9>

[35] K. Bredies, K. Kunisch, and T. Pock, "Total generalized variation," *SIAM Journal on Imaging Sciences*, vol. 3, no. 3, pp. 492–526, Jan. 2010. [Online]. Available: <https://pubs.siam.org/doi/abs/10.1137/090769521>

[36] "U.S. Senate: Roll call votes 112th Congress-2nd session (2010)," Dec. 2010, accessed: 2018-04-18. [Online]. Available: https://www.senate.gov/legislative/LIS/roll_call_lists/vote_menu_111_2.htm

[37] "U.S. Senate: Roll call votes 112th Congress-1st session (2011)," Dec. 2011, accessed: 2018-04-18. [Online]. Available: https://www.senate.gov/legislative/LIS/roll_call_lists/vote_menu_112_1.htm

[38] C. F. Karpowitz, J. Q. Monson, K. D. Patterson, and J. C. Pope, "Tea Time in America? The impact of the Tea Party Movement on the 2010 midterm elections," *PS: Political Science & Politics*, vol. 44, no. 2, pp. 303–309, Apr. 2011.

[39] T. M. J. Fruchterman and E. M. Reingold, "Graph drawing by force-directed placement," *Software: Practice and Experience*, vol. 21, no. 11, pp. 1129–1164, Nov. 1991. [Online]. Available: <http://onlinelibrary.wiley.com/doi/10.1002/spe.4380211102/abstract>

[40] "Arkansas Presidential Election Voting History," <https://www.270towin.com/states/Arkansas>, Apr. 2018. [Online]. Available: <https://www.270towin.com/states/Arkansas>

[41] "Indiana Presidential Election Voting History," <https://www.270towin.com/states/Indiana>, Apr. 2018. [Online]. Available: <https://www.270towin.com/states/Indiana>

[42] V. Williamson, T. Skocpol, and J. Coggins, "The Tea Party and the remaking of Republican conservatism," *Perspectives on Politics*, vol. 9, no. 1, pp. 25–43, Mar. 2011. [Online]. Available: <https://www.cambridge.org/core/journals/perspectives-on-politics/article/tea-party-and-the-remaking-of-republican-conservatism/BDF68005B52758A48F7EC07086C3788C>

[43] B. T. Gervais and I. L. Morris, "Reading the Tea leaves: Understanding Tea Party caucus membership in the US House of Representatives," *PS: Political Science & Politics*, vol. 45, no. 2, pp. 245–250, Apr. 2012.